

RESEARCH ARTICLE

The nature of the Syntaxin4 C-terminus affects Munc18c-supported SNARE assembly

Asma Rehman^{1☯[‡]a}, Shu-Hong Hu^{1☯[‡]ab}, Zakir Tnimov^{2☯[‡]bc}, Andrew E. Whitten^{1^{ad}}, Gordon J. King¹, Russell J. Jarrott^{1^{ab}}, Suzanne J. Norwood², Kirill Alexandrov², Brett M. Collins², Michelle P. Christie^{1^{ae}*}, Jennifer L. Martin^{1^{ab}*}

1 Division of Chemistry and Structural Biology, Institute for Molecular Bioscience, The University of Queensland, St Lucia, Brisbane, QLD, Australia, **2** Division of Cell Biology and Molecular Medicine, Institute for Molecular Bioscience, The University of Queensland, St Lucia, Brisbane, QLD, Australia

☯ These authors contributed equally to this work.

[‡]a Current address: Dulbecco Telethon Institute, Institute of Biophysics, Genova, Italy

[‡]b Current address: Griffith Institute for Drug Discovery, Griffith University, Nathan, QLD, Australia

[‡]c Current address: MRC Laboratory of Molecular Biology, Cambridge, United Kingdom

[‡]d Current address: Australian Nuclear Science and Technology Organisation, Lucas Heights, NSW, Australia

[‡]e Current address: St. Vincent's Institute for Medical Research, Fitzroy, VIC, Australia

* mchristie@svi.edu.au (MPC); jlm@griffith.edu.au (JLM)



OPEN ACCESS

Citation: Rehman A, Hu S-H, Tnimov Z, Whitten AE, King GJ, Jarrott RJ, et al. (2017) The nature of the Syntaxin4 C-terminus affects Munc18c-supported SNARE assembly. PLoS ONE 12(8): e0183366. <https://doi.org/10.1371/journal.pone.0183366>

Editor: Jiajie Diao, University of Cincinnati College of Medicine, UNITED STATES

Received: March 6, 2017

Accepted: August 2, 2017

Published: August 25, 2017

Copyright: © 2017 Rehman et al. This is an open access article distributed under the terms of the [Creative Commons Attribution License](https://creativecommons.org/licenses/by/4.0/), which permits unrestricted use, distribution, and reproduction in any medium, provided the original author and source are credited.

Data Availability Statement: All relevant data are within the paper and its Supporting Information files.

Funding: This work was supported by the Australian National Health and Medical Research Council (NHMRC) program grant 535921 and project grant 1066069. At the time of this work, AEW was supported by an NHMRC Peter Doherty Fellowship (569864); KA was an ARC Future Fellow (FT0991611); BMC was an ARC Future Fellow (FT100100027) and is now an NHMRC Career

Abstract

Vesicular transport of cellular cargo requires targeted membrane fusion and formation of a SNARE protein complex that draws the two apposing fusing membranes together. Insulin-regulated delivery and fusion of glucose transporter-4 storage vesicles at the cell surface is dependent on two key proteins: the SNARE integral membrane protein Syntaxin4 (Sx4) and the soluble regulatory protein Munc18c. Many reported *in vitro* studies of Munc18c:Sx4 interactions and of SNARE complex formation have used soluble Sx4 constructs lacking the native transmembrane domain. As a consequence, the importance of the Sx4 C-terminal anchor remains poorly understood. Here we show that soluble C-terminally truncated Sx4 dissociates more rapidly from Munc18c than Sx4 where the C-terminal transmembrane domain is replaced with a T4-lysozyme fusion. We also show that Munc18c appears to inhibit SNARE complex formation when soluble C-terminally truncated Sx4 is used but does not inhibit SNARE complex formation when Sx4 is C-terminally anchored (by a C-terminal His-tag bound to resin, by a C-terminal T4L fusion or by the native C-terminal transmembrane domain in detergent micelles). We conclude that the C-terminus of Sx4 is critical for its interaction with Munc18c, and that the reported inhibitory role of Munc18c may be an artifact of experimental design. These results support the notion that a primary role of Munc18c is to support SNARE complex formation and membrane fusion.

Introduction

Vesicular trafficking in eukaryotic cells depends on targeted fusion reactions between vesicles and their specific target membranes. Two universally required components of the intracellular

Development Fellow (APP1061574); and JLM was an ARC Australian Laureate Fellow (FL0992138) and honorary NHMRC Fellow (APP455829). The funders had no role in study design, data collection and analysis, decision to publish, or preparation of the manuscript.

Competing interests: The authors have declared that no competing interests exist.

membrane fusion machinery are soluble N-ethylmaleimide-sensitive factor attachment protein receptor (SNARE) proteins and Sec1/Munc18 (SM) proteins. Target membrane (*t*-) SNAREs, anchored to one membrane, form a molecular zipper with cognate vesicle (*v*-) SNAREs on a vesicle membrane generating an α -helical bundle that pulls the two membranes together and drives fusion [1–3].

Vesicular transport is dependent on SNARE complex assembly, which is regulated by SM proteins [4, 5]. Thus, delivery of the glucose transporter-4 (GLUT4) to the cell membrane in response to insulin signaling requires the SM protein Munc18c as well as two *t*-SNAREs (Syntaxin4 (Sx4), SNAP23) [6, 7] and the *v*-SNARE (VAMP2/syntaxin4) [8]. Knockouts and overexpression of SM proteins have shown both positive and negative effects on SNARE complex assembly and vesicle fusion [9, 10], and there is little agreement on the precise role of SM proteins.

Three isoforms of SM proteins have been identified for exocytosis events in mammals: Munc18a (also known as Munc18-1), Munc18b (Munc18-2) and Munc18c (Munc18-3) [7, 11]. Each Munc18 protein interacts with a cognate Syntaxin (Sx) protein composed of an N-peptide (a 10–30 residue region at the N-terminus) followed by an α -helical bundle (the H_{abc} domain), a SNARE motif, and a C-terminal transmembrane region. The best-studied Munc18:Sx interaction is that between Munc18a and Syntaxin1a (Sx1a); both are required for synaptic vesicle-mediated neurotransmitter release [2, 12, 13]. Munc18a interacts with Sx1a with nanomolar affinity [14–18] and two alternate binding modes have been described. The first involves Munc18a interacting with a “closed” 4-helix bundle conformation of Sx1a (where the SNARE helix is sequestered by the H_{abc} domain). This Munc18a:Sx1a closed binding mode is consistent with a negative regulatory role for Munc18a, because the SNARE helix is unable to interact with partner SNAREs to drive vesicle fusion [15, 16, 18–20]. A second Munc18a:Sx1a binding mode occurs when Munc18a associates with the SNARE ternary complex in which Sx1a adopts an “open” conformation [17, 21–26]. While the neuronal Munc18a:Sx1a complex is reported to form closed “fusion-incompetent” and open “fusion-competent” conformations, the closely related Munc18c:Sx4 system appears to use only the open Sx4 binding mode [17, 27, 28], though this remains controversial. Indeed, the closed binding mode interaction of Sx1a with Munc18a has been suggested to be a specialization of the neuronal exocytotic pathways [29].

In the cell, Sxs are anchored by a C-terminal transmembrane helix to the plasma membrane, providing an anchor for the adjoining SNARE helix (Fig 1A). Furthermore, a crystal structure of the neuronal SNARE complex shows that the C-terminal transmembrane domains of Sx1a and VAMP2 form continuous α -helices with their SNARE motifs [30]. This finding suggests that the transmembrane domain is not only an anchor but may also play an integral part in the protein structure. However, *in vitro* experiments designed to study Munc18:Sx interactions, both in the neuronal and GLUT4 systems, have generally used truncated Sxs, including soluble Sx lacking its C-terminal membrane anchor [15, 18], soluble truncated Sx immobilized at its N-terminus (with the SNARE helix untethered) [31] or soluble Sx immobilized at its C-terminus [17, 25, 28]. Other reports have used full-length Sxs incorporated into proteoliposomes through native C-terminal membrane anchors [23, 24, 27, 32–36]. Based on the conclusions derived from these experiments we postulated that the nature of the Sx4 C-terminus affects the observed *in vitro* activity of Munc18c [37]. Here, we test the hypothesis that experimental design—specifically focusing on the Sx4 C-terminus—influences the observed effect of Munc18c on SNARE assembly. We show that when the Sx4 C-terminus is anchored, SNARE assembly occurs in the presence of Munc18c yet when the Sx4 C-terminus is not anchored SNARE assembly is inhibited in the presence of Munc18c.

Results

To investigate whether anchoring of the Sx4 C-terminus has an effect on SNARE complex assembly in the presence of Munc18c, we designed several Sx4 constructs including: the soluble cytoplasmic domain (Sx4₁₋₂₇₅); a Sx4 construct containing the soluble cytoplasmic domain with a

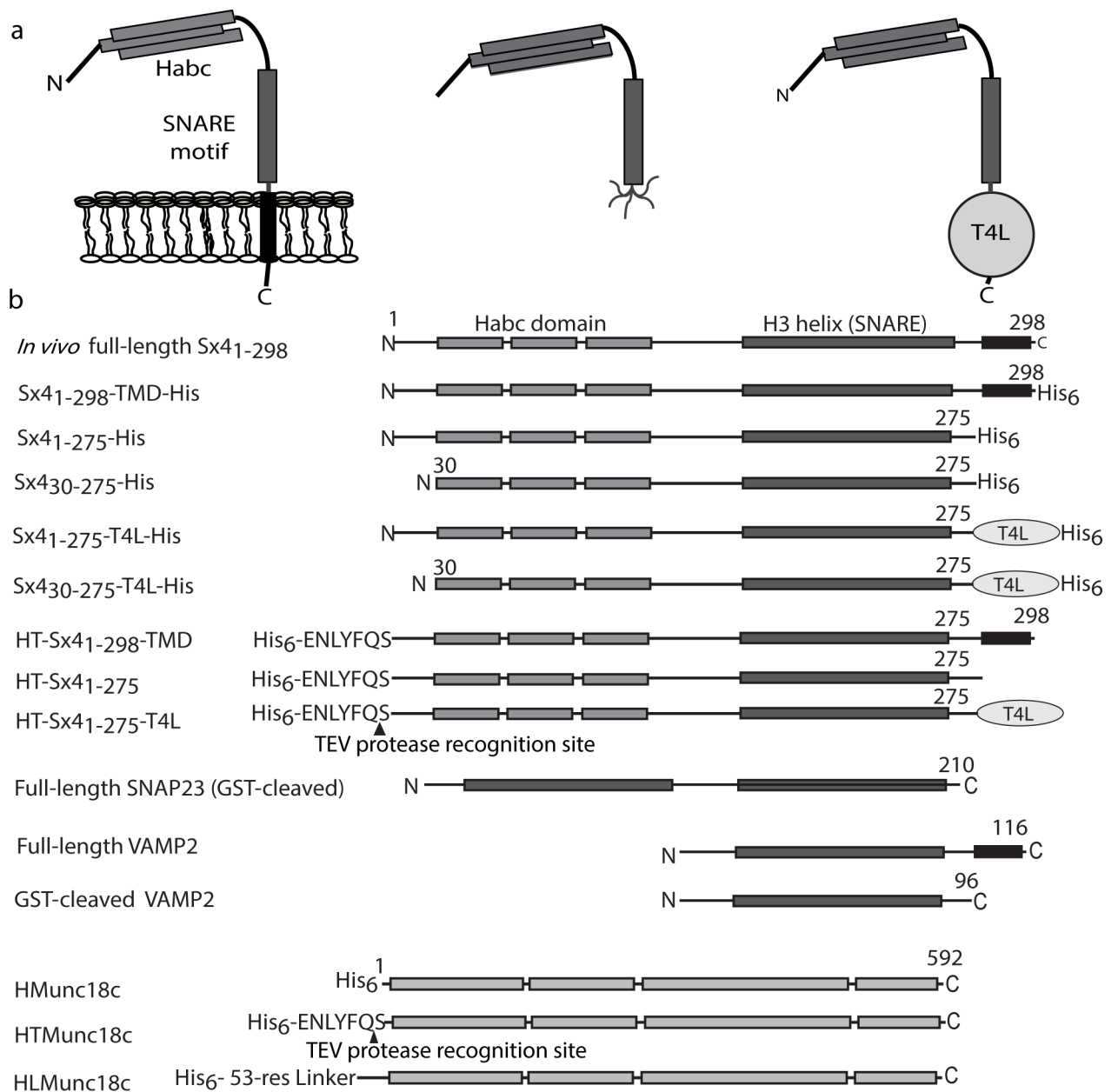


Fig 1. Schematic of protein constructs used in this study. **a.** *In vivo* full-length Sx4₁₋₂₉₈ consists of an N-terminal peptide, an α -helical bundle (the H_{abc} domain), a SNARE motif and a C-terminal transmembrane domain. Without the transmembrane domain Sx4 is no longer associated with a membrane and the Sx4 SNARE helix is also likely to be flexible when it is not anchored. We investigated the effect of anchoring the Sx4 C-terminus by using full-length Sx4 including the transmembrane domain, soluble Sx4 lacking the transmembrane domain and soluble Sx4 with a C-terminal T4 lysozyme (T4L) fusion. **b.** Schematic representation of all protein constructs used in this study, illustrating the position of engineered fusion tags and protease cleavage sites. For Sx4 constructs, His indicates a C-terminal hexahistidine (His₆) tag, TMD indicates a C-terminal transmembrane domain, HT indicates an N-terminal His₆ tag with a TEV protease recognition site. For Munc18c, H indicates an N-terminal His₆ tag, HT indicates an N-terminal His₆ tag with a TEV protease recognition site, HL indicates an N-terminal His₆ tag with a long linker. SNAP23 and VAMP2 proteins used in this study are the constructs labeled GST-cleaved in this figure.

<https://doi.org/10.1371/journal.pone.0183366.g001>

C-terminal fusion protein T4-lysozyme (Sx4₁₋₂₇₅-T4L); and the full-length protein complete with C-terminal transmembrane domain helix (Sx4₁₋₂₉₈-TMD). We hypothesized that C-terminal anchoring of the Sx4 constructs may mimic the *in vivo* situation where Sx4 is inserted into the plasma membrane by its C-terminal transmembrane helix. The Sx4₁₋₂₇₅-T4L protein fusion was included as a way of reducing the Sx4 C-terminal flexibility that is likely to occur when the transmembrane domain is removed, and potentially structure the otherwise disordered C-terminal region in Sx4₁₋₂₇₅ [17]. A similar strategy has been used successfully to decrease the flexibility of loops and termini in GPCR research [38]. A range of Sx4 constructs were engineered with either a C-terminal His₆-tag for purification and immobilization on metal affinity resin, or a TEV-cleavable N-terminal His₆-tag for the production of de-tagged Sx4 proteins. The Sx4, Munc18c, SNAP23 and VAMP2 constructs used in this work are shown schematically in Fig 1B.

C-terminally anchored Sx4 with a T4L fusion forms a complex with Munc18c

We undertook pulldown experiments to investigate if the Sx4₁₋₂₇₅-T4L construct behaved similarly to Sx4₁₋₂₇₅. Sx4 constructs were immobilized via their C-terminal His₆-tag onto metal affinity resin, so that all Sx4 constructs were similarly bound by their C-terminus. The results of these experiments clearly show that Munc18c binds to both C-terminally immobilized Sx4 proteins Sx4₁₋₂₇₅-His and Sx4₁₋₂₇₅-T4L-His (Fig 2). Importantly, only a very small amount of Munc18c was pulled down in the negative control (labeled Munc18c), confirming that the binding of Munc18c was specific to Sx4. Moreover, no Munc18c above the negative control levels was pulled down by Sx4₃₀₋₂₇₅-T4L-His, consistent with previous observations that binding of Munc18c to Sx4 requires the Sx4 N-terminal residues (the Syntaxin N-peptide) [17, 28].

The importance of the Sx4 N-peptide for binding to Munc18c was confirmed once again using ITC, where binding was detected for HMunc18c (Munc18c with an N-terminal His₆-tag) and Sx4₁₋₂₇₅-T4L-His, but not for HMunc18c and Sx4₃₀₋₂₇₅-T4L-His (S1 Table). The ITC determined binding affinity, K_d , of 100 nM for the HMunc18c:Sx4₁₋₂₇₅-T4L-His interaction (S1 Table, S1 Fig) is similar to that reported previously for the interaction between Munc18c and Sx4₁₋₂₇₅-His (K_d 95–104 nM) [17, 39]. These results indicate that the T4L fusion does not affect the binding affinity of Sx4 for Munc18c.

C-terminal anchoring of Sx4 slows dissociation from Munc18c

To assess more quantitatively the effect of anchoring the C-terminus of Sx4, we assayed Munc18c interactions with Sx4 constructs using bio-layer interferometry. When Sx4 constructs were immobilized via their C-terminal His₆-tag onto Ni-NTA biosensors, both Sx4 variants—Sx4₁₋₂₇₅-His and Sx4₁₋₂₇₅-T4L-His—had similar association rate constants (k_{on} , $M^{-1}s^{-1}$), dissociation rate constants (off-rates, k_{off} , s^{-1}) and binding affinities (Table 1, S2 Fig) for detagged Munc18c. In the reverse experiment, HLMunc18c was immobilized. In this case, Sx4₁₋₂₇₅-T4L (K_d = 31 nM) bound to HLMunc18c with a higher affinity than Sx4₁₋₂₇₅ (K_d = 72 nM). Further analysis showed that the two pairs of proteins had similar association rate constants, but that the dissociation rate constant for HLMunc18c:Sx4₁₋₂₇₅ was ~2.5 times faster than for HLMunc18c:Sx4₁₋₂₇₅-T4L demonstrating a weaker association for the former.

We then investigated these same pairs of interactions by fluorescence anisotropy where neither protein is immobilized. The Sx4 proteins (Sx4₁₋₂₇₅-His, Sx4₁₋₂₇₅-T4L-His) were labeled with the Alexa Fluor® 488 maleimide probe (see Materials and Methods) and kinetic titrations of the labeled Sx4 proteins (each at 50 nM) were measured with increasing concentrations of HMunc18c. Addition of HMunc18c to the Alexa488-labeled Sx4₁₋₂₇₅-His or Sx4₁₋₂₇₅-T4L-His resulted in an increase in fluorescence anisotropy indicating formation of Munc18c

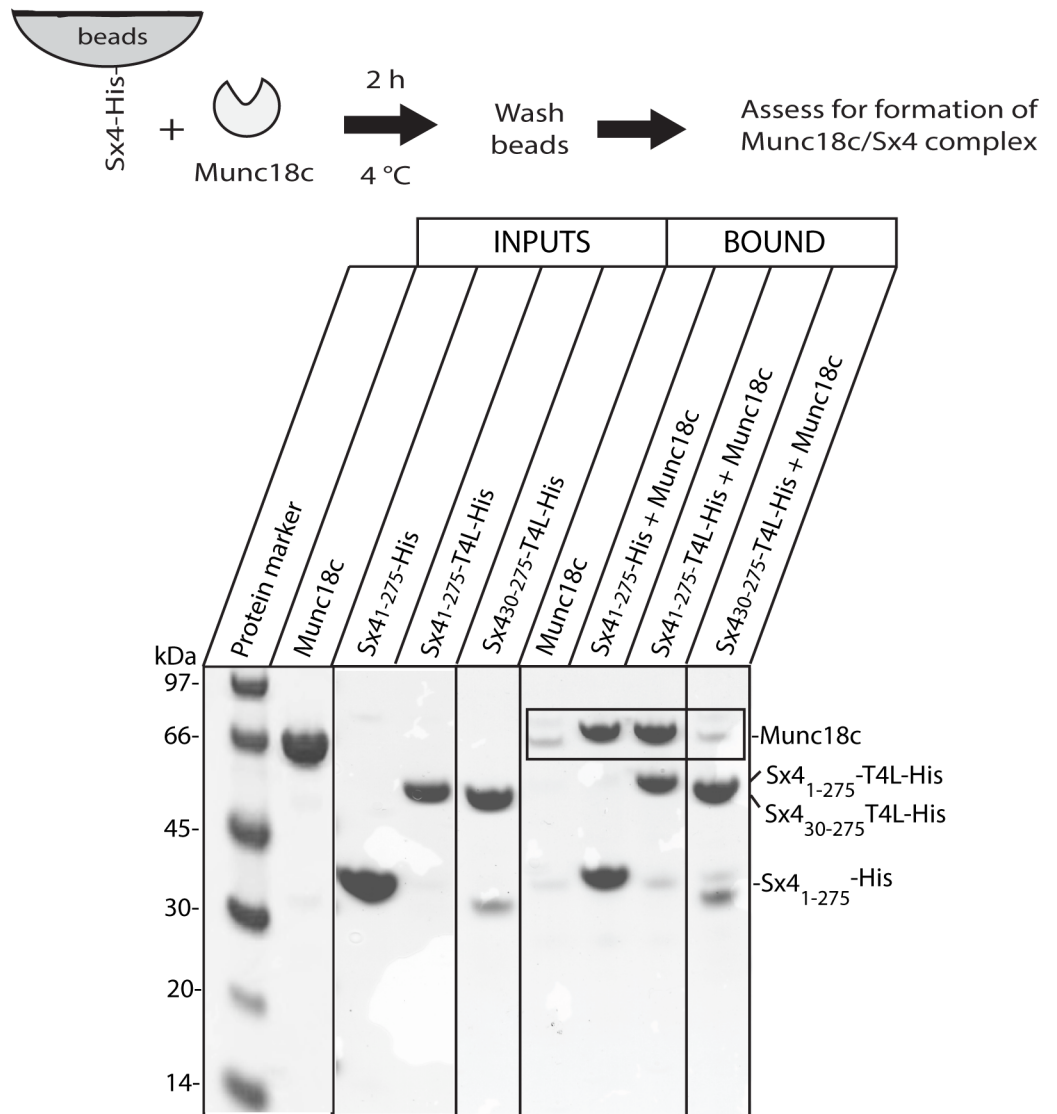


Fig 2. Munc18c binds to Sx4 proteins immobilized by their C-terminus onto beads. Coomassie Blue stained SDS-PAGE gel showing that (after a 2 hr incubation at 4°C) de-tagged Munc18c is pulled down by all Sx4 proteins immobilized by their C-terminus, except Sx4₃₀₋₂₇₅-T4L which lacks the N-peptide sequence known to be important for Munc18c binding. There was negligible non-specific binding of de-tagged Munc18c to the metal affinity resin (lane labeled Bound, Munc18c). The expected position of Munc18c on the gel is boxed. The gel displayed is representative of three replicate experiments. Solid vertical lines on the gel image indicate the removal of intervening lanes.

<https://doi.org/10.1371/journal.pone.0183366.g002>

complexes with both Sx4 variants (Fig 3A and 3B). The T4L fusion did not greatly affect the association rate constant. In contrast, the dissociation rate constant (k_{off} s⁻¹) of HMunc18c: Sx4₁₋₂₇₅-His was almost an order of magnitude faster than that of HMunc18c: Sx4₁₋₂₇₅-T4L-His (Table 1). These results are consistent with the outcomes from the bio-layer interferometry experiments and support the notion that the nature of the Sx4 C-terminus affects dissociation kinetics with Munc18c.

In combination, these results show that anchoring the C-terminus of Sx4 (either by using a C-terminal His-tag anchored to affinity resin or by using a C-terminal T4L fusion) slows dissociation of Sx4 from Munc18c, although the mechanism for this is unclear.

Table 1. Summary of kinetic data for the Munc18c-Syntaxin4 interaction. Values shown for the bio-layer interferometry experiments are mean \pm s.d. where each experiment was repeated at least three times. Values and standard errors are shown for the fluorescence anisotropy experiments and these were obtained from a global fit to multiple kinetic data sets with differing concentrations of Munc18c. Bold text indicates dissociation rate constants (k_{off}) for Munc18c-Sx4₁₋₂₇₅ where Sx4₁₋₂₇₅ is free in solution.

Sx4 construct	Experimental design		$k_{on}, M^{-1}s^{-1}$	k_{off}, s^{-1}	K_d, nM
	Sx4	Munc18c			
Bio-layer interferometry					
Sx4 ₁₋₂₇₅ -His	Immobilized	In solution	$(5.3 \pm 2.6) \times 10^5$	$(8.6 \pm 1.1) \times 10^{-3}$	21 ± 13
Sx4 ₁₋₂₇₅ -T4L-His	Immobilized	In solution	$(4.3 \pm 1.8) \times 10^5$	$(7.8 \pm 2.5) \times 10^{-3}$	20 ± 7
Sx4 ₁₋₂₇₅	In solution	Immobilized	$(3.0 \pm 0.7) \times 10^5$	$(22 \pm 8) \times 10^{-3}$	72 ± 16
Sx4 ₁₋₂₇₅ -T4L	In solution	Immobilized	$(2.9 \pm 0.4) \times 10^5$	$(9.0 \pm 1.2) \times 10^{-3}$	31 ± 6
Fluorescence Anisotropy					
Sx4 ₁₋₂₇₅ -His	In solution	In solution	$(1.30 \pm 0.04) \times 10^3$	$(65.3 \pm 0.4) \times 10^{-5}$	502 ± 16
Sx4 ₁₋₂₇₅ -T4L-His	In solution	In solution	$(5.02 \pm 0.13) \times 10^2$	$(7.5 \pm 0.4) \times 10^{-5}$	148 ± 9

<https://doi.org/10.1371/journal.pone.0183366.t001>

Sx4 C-terminal anchoring promotes SNARE assembly in the presence of Munc18c

We next investigated the effect of Sx4 C-terminal anchoring on the impact of Munc18c-mediated SNARE complex assembly. Using a pull-down assay, we explored the ability of Sx4 variants (Sx4₁₋₂₇₅-His and Sx4₁₋₂₇₅-T4L-His) to bind SNARE partners. Both Sx4 constructs, when immobilized on metal affinity resin by their C-terminal His₆-tags in a pre-formed complex with Munc18c, were able to pull down SNAP23 and VAMP2 to form SNARE complexes after overnight incubation (Fig 4).

The importance of Sx4 C-terminal anchoring on SNARE complex assembly was then examined by using a pre-formed binary complex between immobilized HL-Munc18c and de-tagged Sx4 constructs in SNARE pull-down experiments (Fig 5). HL-Munc18c was first immobilized onto beads, then Sx4 proteins were pulled down. For this critical experiment, we used detagged Sx4₁₋₂₇₅, Sx4₁₋₂₇₅-T4L and the full-length Sx4₁₋₂₉₈.TMD (in detergent micelles). After extensive

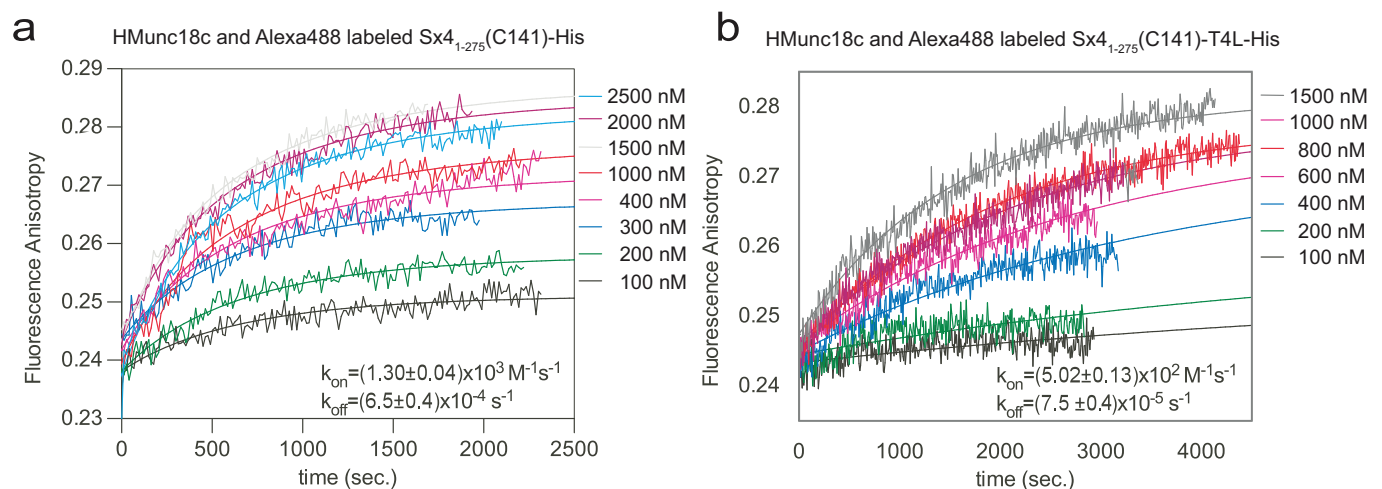


Fig 3. Kinetics of Munc18c interaction with Sx4 in solution. **a.** Time course of complex formation of Alexa488-labeled Sx4₁₋₂₇₅-His (50 nM) with HMunc18c at various concentrations: 100 nM (black curve), 200 nM (green curve), 300 nM (blue curve), 400 nM (pink curve), 1000 nM (red curve), 1500 nM (grey curve), 2000 nM (magenta curve) and 2500 nM (cyan curve). Solid lines represent global fits to titration data in the Dynafit 4.0 program. Resulting kinetic constants are shown in the graph inset. **b.** As for **a.** except that formation of HMunc18c:Sx4₁₋₂₇₅-T4L-His was monitored. Concentrations of HMunc18c used were: 100 nM (black curve), 200 nM (green curve), 400 nM (blue curve), 600 nM (pink curve), 800 nM (red curve), 1000 nM (magenta curve), 1500 nM (gray curve).

<https://doi.org/10.1371/journal.pone.0183366.g003>

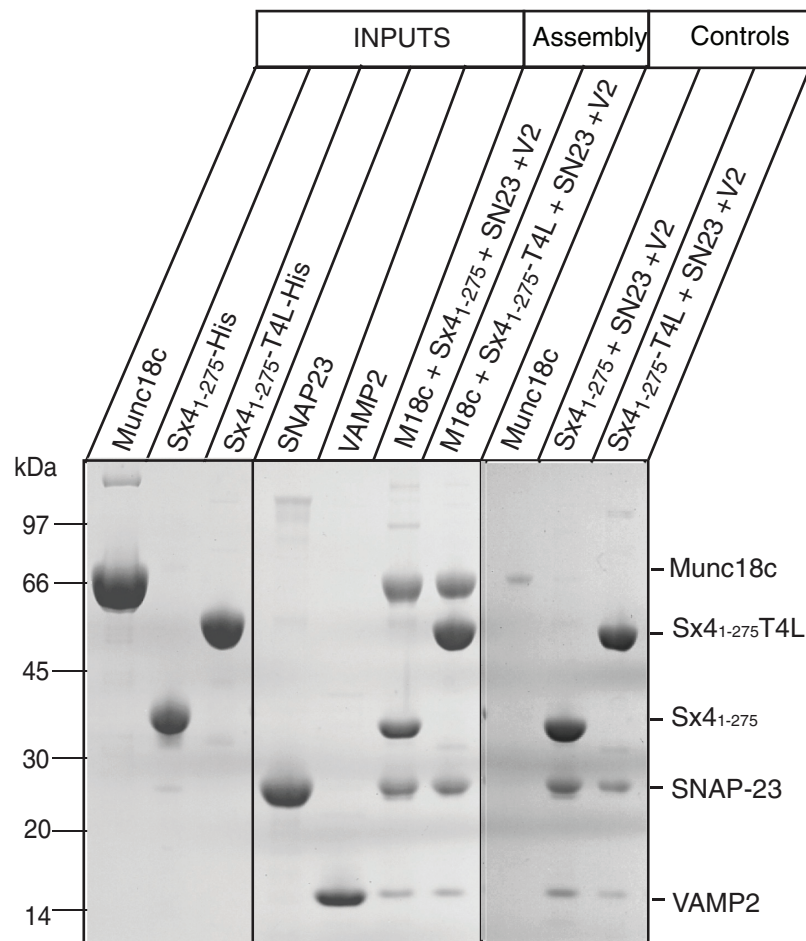
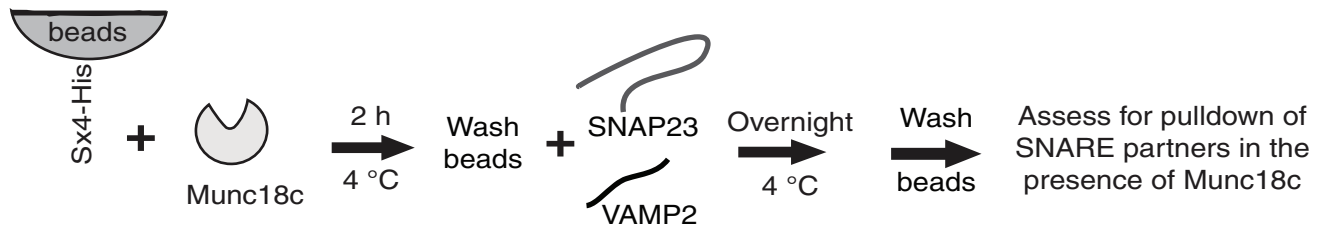


Fig 4. Munc18c does not block SNARE assembly when the Sx4 C-terminus is immobilized. Coomassie Blue stained SDS-PAGE analysis of the binding of SNAP23 and VAMP2 to Sx4 proteins (Sx4₁₋₂₇₅-His or Sx4₁₋₂₇₅-T4L-His) immobilized on Co²⁺resin by their C-terminus. Immobilized Sx4 proteins were complexed with Munc18c (de-tagged) prior to overnight incubation with SNAP23 and VAMP2. C-terminally immobilized Sx4 proteins were able to pull down SNARE partners (SNAP23 and VAMP2) in the presence of Munc18c (lanes labeled Assembly) and in the absence of Munc18c (lanes labeled Controls). Lanes labeled INPUTS show the protein samples used in the experiments. The control lane labeled Munc18c is a negative control showing the lack of interaction of Munc18c with beads. The gel displayed is representative of three replicate experiments. Solid vertical lines on the gel image indicate the removal of intervening lanes or where two different gels have been placed adjacent to each other.

<https://doi.org/10.1371/journal.pone.0183366.g004>

washing to remove unbound Sx4 proteins, the beads were incubated with SNARE partner proteins (SNAP23 and VAMP2). We found that when bound to HL-Munc18c, both Sx4₁₋₂₇₅-T4L and Sx4₁₋₂₉₈-TMD were able to assemble ternary complex by pulling down SNAP23 and VAMP2, whereas Sx4₁₋₂₇₅ did not (Fig 5). The experiments were repeated four times, including the use of different batches of each purified protein. In each experiment, the results were

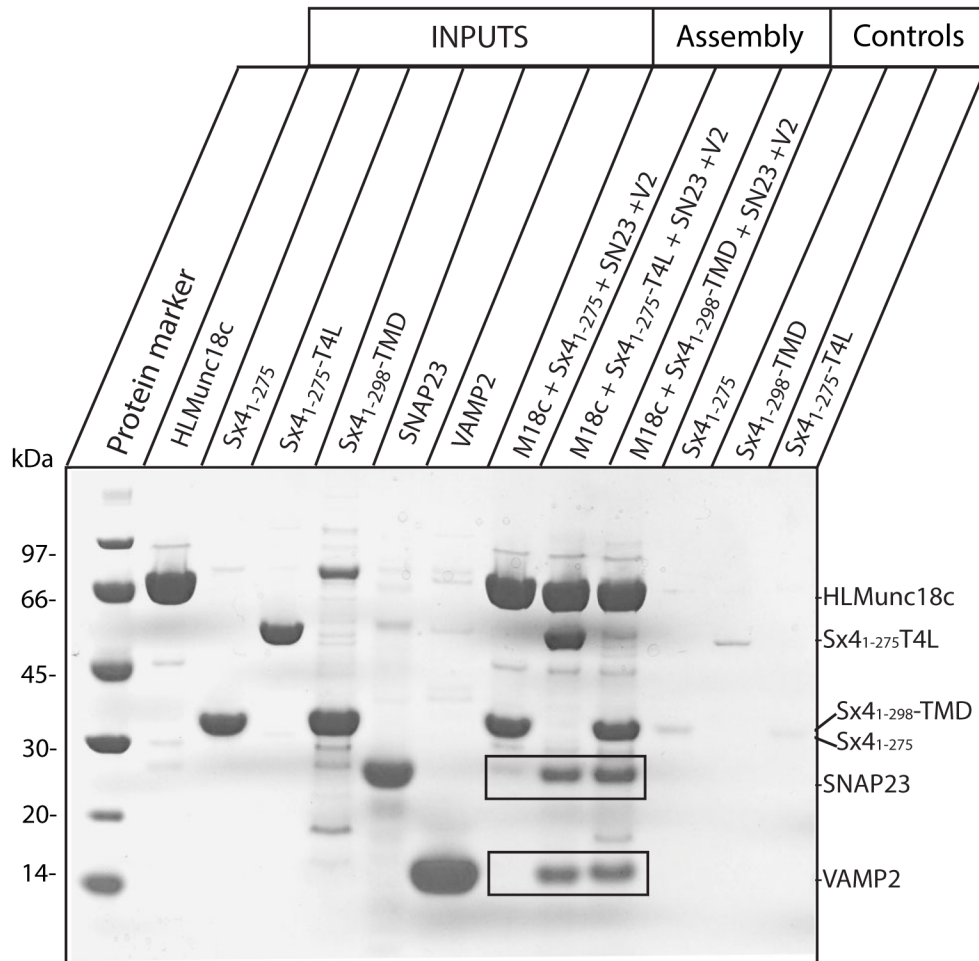
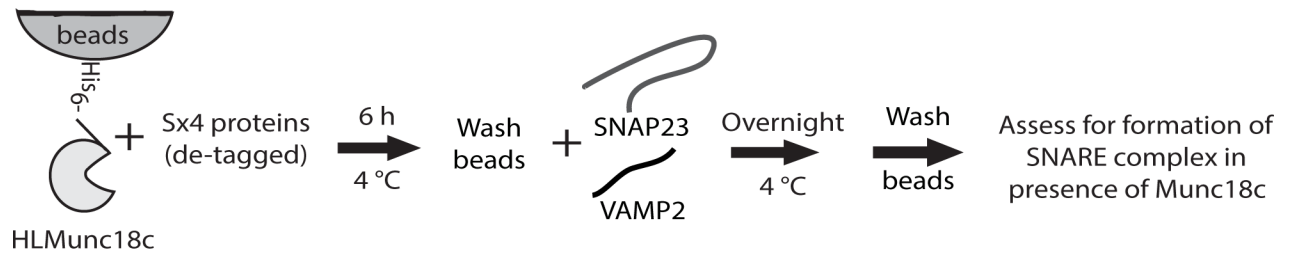


Fig 5. Munc18c prevents SNARE assembly when Sx4 C-terminus is not immobilized. Coomassie Blue stained SDS-PAGE analysis of the binding of SNAP23 and VAMP2 to Sx4s (de-tagged Sx4₁₋₂₇₅, Sx4₁₋₂₇₅-T4L or Sx4₁₋₂₉₈-TMD) bound to HL-Munc18c. HL-Munc18c was immobilized on Co²⁺ resin and incubated for 6 h with Sx4₁₋₂₇₅, Sx4₁₋₂₇₅-T4L or Sx4₁₋₂₉₈-TMD and then allowed to interact with SNAP23 and VAMP2 overnight. The gel shows that SNAP23 and VAMP2 were pulled down by Munc18c:Sx4₁₋₂₇₅-T4L and Munc18c:Sx4₁₋₂₉₈-TMD but not by Munc18c:Sx4₁₋₂₇₅. The expected positions of pulled down SNAP23 and VAMP2 proteins are boxed. The gel displayed is representative of four replicate experiments. Lanes labeled INPUTS show the protein samples used in the experiments. Lanes labeled Controls, show that Sx4₁₋₂₇₅, Sx4₁₋₂₇₅-T4L or Sx4₁₋₂₉₈-TMD do not bind to the Co²⁺ resin in the absence of bound HL-Munc18c.

<https://doi.org/10.1371/journal.pone.0183366.g005>

the same. This result shows that SNAP23 and VAMP2 are pulled down only when Munc18c is in complex with a Sx4 construct that has a C-terminal anchor. Pull-down experiments using T4L-His immobilized on beads showed negligible binding of SNAP23 or VAMP2 (S3 Fig) indicating that the capture of these two proteins (in the experiment presented in Fig 5) is due to interaction with Sx4 and not with T4L.

Table 2. Observed rate constants (k_{obs} , s^{-1}) of SNARE complex formation measured by fluorescence anisotropy (VAMP2 labeled) for Sx4 constructs in the presence and absence of Munc18c. Values are shown as mean $k_{obs} \pm$ s.d. from three independent experiments. Bold text indicates the observed rate constant (k_{obs}) for Sx4₁₋₂₇₅ SNARE assembly in the absence and presence of Munc18c showing that SNARE assembly is 7-fold slower in the presence of Munc18c for this construct only. Shading indicates all four experiments for which Munc18c was included, showing that Munc18c did not inhibit SNARE assembly when the Sx4 C-terminus had a T4L fusion, or when the Sx4 N-peptide was removed.

Protein interaction partners	k_{obs} , s^{-1}
Sx4₁₋₂₇₅-His SNARE assembly	$(4.9 \pm 0.9) \times 10^{-4}$
Sx4 ₁₋₂₇₅ -T4L-His SNARE assembly	$(5.0 \pm 1.0) \times 10^{-4}$
Sx4 ₃₀₋₂₇₅ -His SNARE assembly	$(4.9 \pm 1.4) \times 10^{-4}$
Sx4 ₃₀₋₂₇₅ -T4L-His SNARE assembly	$(4.8 \pm 1.7) \times 10^{-4}$
Sx4₁₋₂₇₅-His SNARE assembly + HMunc18c	$(0.7 \pm 0.4) \times 10^{-4}$
Sx4 ₁₋₂₇₅ -T4L-His SNARE assembly + HMunc18c	$(5.1 \pm 1.1) \times 10^{-4}$
Sx4 ₃₀₋₂₇₅ -His SNARE assembly + HMunc18c	$(4.8 \pm 0.6) \times 10^{-4}$
Sx4 ₃₀₋₂₇₅ -T4L-His SNARE assembly + HMunc18c	$(5.0 \pm 0.8) \times 10^{-4}$

<https://doi.org/10.1371/journal.pone.0183366.t002>

Munc18c only inhibits SNARE assembly when Sx4 C-terminus is not anchored

To assess the role of Munc18c in SNARE complex formation when each cognate SNARE and SM protein is free in solution, we made use of a fluorescence anisotropy assay that has been used previously to assess neuronal SNARE assembly [15, 18]. In the previously reported work, SNARE complex formation using the soluble cytoplasmic form of neuronal Sx1a (Sx1a₁₋₂₆₂) was inhibited in the presence of Munc18a. To gain insight into the importance of the Sx4 C-terminus, our experiments were designed to evaluate whether the same result occurs for Sx4₁₋₂₇₅ (analogous to the cytoplasmic Sx1a₁₋₂₆₂ construct) and whether this result changes when the C-terminus is fused to T4L (Sx4₁₋₂₇₅-T4L).

SNARE complex formation was monitored by the change in fluorescence anisotropy of Alexa488 labeled VAMP2 in the presence or absence of Munc18c. In the absence of Munc18c, SNARE ternary complex was formed in the presence of both Sx4₁₋₂₇₅-His and Sx4₁₋₂₇₅-T4L-His at almost the same rates (Table 2). In contrast, the rate of SNARE complex formation for Sx4₁₋₂₇₅-His in the presence of HMunc18c is 7-fold lower than for Sx4₁₋₂₇₅-His alone (Table 2, Fig 6A). These findings for Munc18c are in agreement with the results of previous studies on neuronal counterparts [15, 16, 18] that showed Munc18a inhibited assembly of Sx1a₁₋₂₆₂ SNARE complexes in solution.

When we conducted the same experiment using Sx4₁₋₂₇₅-T4L-His the rate of SNARE complex formation is unchanged by the addition of HMunc18c (Table 2, Fig 6B). This outcome is in line with the results reported above from pull-down assays where Sx4₁₋₂₇₅-T4L or Sx4₁₋₂₉₈-TMD bound to immobilized HLMunc18c were able to pull down SNARE partners, whereas Sx4₁₋₂₇₅ bound to Munc18c failed to form SNARE complexes unless the Sx4₁₋₂₇₅ was C-terminally immobilized on beads.

Removing the Sx4 N-peptide releases the effect of Munc18c on SNARE assembly

To assess whether the N-terminal peptide of Sx4 plays a role in SNARE assembly, we performed fluorescence anisotropy experiments analogous to those reported previously for Munc18a:Sx1a [18]. We studied complex formation for Sx4₃₀₋₂₇₅ in the presence or absence of Munc18c (Table 2, Fig 6C). We also analyzed SNARE complex formation using Sx4₃₀₋₂₇₅-T4L

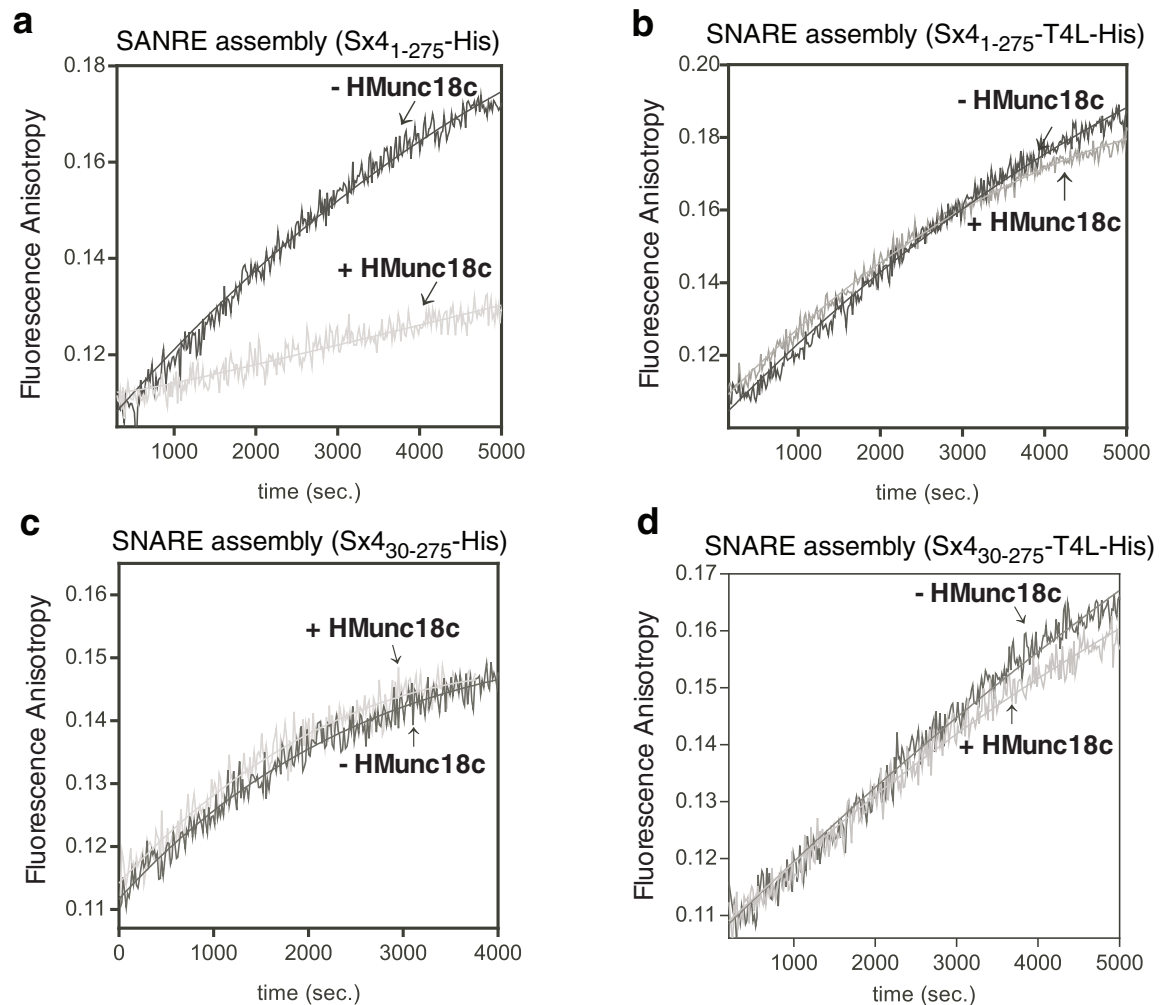


Fig 6. Munc18c reduces the rate of SNARE complex formation in solution when the Sx4 C-terminus is not anchored. Panels **a**. Sx4₁₋₂₇₅-His, **b**. Sx4₁₋₂₇₅-T4L-His, **c**. Sx4₃₀₋₂₇₅-His and **d**. Sx4₃₀₋₂₇₅-T4L-His show typical fluorescence anisotropy traces upon mixing SNARE complex components: 700 nM SNAP23, 100 nM Alexa488-labeled VAMP2 and 700 nM Sx4-variant alone (dark gray) or in the presence of 500 nM Munc18c (light gray).

<https://doi.org/10.1371/journal.pone.0183366.g006>

(having a C-terminal fusion) in the presence and absence of Munc18c. The rate of SNARE assembly in the absence of Munc18c is similar for Sx4₃₀₋₂₇₅ and Sx4₁₋₂₇₅ (Table 2) indicating that the presence of the N-peptide does not affect the interaction with SNARE partners. However there is a marked difference in the rate of SNARE assembly for Sx4₃₀₋₂₇₅ and Sx4₁₋₂₇₅ (i.e. without and with N-peptide) in the presence of Munc18c. For Sx4₁₋₂₇₅, SNARE assembly is reduced by 7-fold in the presence of Munc18c. For Sx4₃₀₋₂₇₅ there is no significant rate reduction of SNARE assembly in the presence of Munc18c (Table 2, Fig 6C). When the C-terminal Sx4₃₀₋₂₇₅-T4L fusion protein is used, there is again no difference observed in the rate of SNARE assembly in the presence of Munc18c (Table 2, Fig 6D). Indeed, for Sx4s lacking N-terminal residues, SNARE assembly in solution proceeds at very similar rates whether or not the Sx4 C-terminus is fused to T4L and whether or not Munc18c is present. We note that Sx4₃₀₋₂₇₅ binds very weakly, if at all, to Munc18c [17] (Fig 3, S1 Table), so that SNARE assembly for this construct probably does not involve Munc18c. Thus the “release” of Munc18c

inhibition observed when the N-peptide of Sx4 is removed, may simply be a consequence of Munc18c not participating in SNARE assembly.

Discussion

Previously reported *in vitro* evidence for the role of Munc18c has been used to support both positive [27, 28] and negative [32, 40] regulatory roles on SNARE assembly. This situation is mirrored for the neuronal counterpart Munc18a [15, 16, 18, 19, 21–27, 33, 34, 41]. We questioned whether these contradictory conclusions for the role of Munc18c - derived from *in vitro* experiments—could be a consequence of experimental design.

Removing the Sx4 C-terminus would have two immediately apparent effects: first, Sx4 would not be associated with a membrane; and, second, the Sx4 SNARE region would not be anchored at its C-terminus and its C-terminal residues would be less ordered/more flexible. Indeed, a crystal structure of the C-terminally truncated Sx1 in complex with Munc18a revealed that the C-terminal region of Sx1 was disordered [42]. Similarly, the SNARE region of a soluble C-terminally truncated Sx1 construct was flexible [17, 43]. On the other hand, a crystal structure of the neuronal SNARE complex that includes the Sx1 and VAMP2 C-terminal transmembrane domains showed a continuous helical structure for the SNARE motifs and TMD domains [30]. Moreover, NMR analysis of Sx1 including the transmembrane domain in micelles showed two well-ordered helices in the SNARE domain and a well-ordered helix in the transmembrane region [44]. Together this evidence supports the conjecture that removing the transmembrane anchor of Sxs could affect the C-terminal SNARE structure. Here we investigated whether this effect might impact on the outcome of *in vitro* SNARE assembly experiments.

Using multiple lines of evidence, we found a consistent relationship. In essence, different experimental designs give rise to contradictory conclusions on the role of Munc18c in SNARE assembly. Strategies in which the Sx4 C-terminus is attached to beads in *in vitro* pull-down assays show that Munc18c does not inhibit SNARE assembly. Conversely, strategies in which Sx4 is not immobilized by its C-terminus or is free in solution show that SNARE assembly is inhibited when C-terminally truncated Sx4 is used, but not when using Sx4 that includes its TMD, or when fused to T4L. The *in vitro* experimental design using a C-terminal anchor (T4L or TMD in a detergent micelle) does not include a membrane bilayer, but nevertheless the outcomes closely resemble those reported for Sx4 reconstituted in liposomes [27].

Unlike neuronal Munc18a, Munc18c is thought to only bind Sx4 in an open conformation [17, 27]. The inclusion of a Sx4 C-terminal anchor in *in vitro* experiments may enable a conformation of Sx4 in the Munc18c:Sx4 complex that can also accommodate SNAP23 and VAMP2 binding. This finding is of critical importance in the field, and explains conflicting conclusions from studies of the role of Munc18c in promoting SNARE assembly. In its native form Sx4 is membrane-embedded. Our results thus provide compelling evidence that Munc18c does not inhibit SNARE assembly *in vivo*. We reason that the negative regulatory role ascribed to Munc18c is artifactual and is a consequence of using soluble truncated Sx4. However, further experiments will now be required to define the precise role of the Sx4 C-terminal region in modulating Munc18c/SNARE interactions.

More broadly, our findings suggest that experimental design and interpretation of *in vitro* data should perhaps be revisited for other vesicle fusion systems. We note, for example, that *in vivo* studies using Sx1 with a lipidic anchor in place of the transmembrane helix fully supported fusion, but that distancing the SNARE motif from the membrane inhibits membrane fusion [45], in support of our model. Our findings suggest that the most appropriate Sx construct to use for *in vitro* experiments with Munc18 partners is the membrane-anchored form or, failing that, Sx with a C-terminal tag attached to affinity beads, or a C-terminal fusion such as T4L.

In summary, our data show that Munc18c only has an inhibitory effect on SNARE assembly when the Sx4 C-terminus is removed. Because native Sx4 is anchored by its C-terminus to the plasma membrane, we conclude that Munc18c almost certainly does not block native Sx4 SNARE assembly *in vivo*. Other membrane fusion components may exert complex regulatory control in these exquisitely organized trafficking systems, including a wide range of positive and negative regulation of Munc18 proteins by a wide range of mechanisms. Finally, our findings call into question the common practice of removing transmembrane anchors to study protein interactions when the interacting region of the protein adjoins the transmembrane helix.

Materials and methods

Constructs

Plasmids encoding rat Sx4 (C141S, amino acids 1–275), with a C-terminal hexahistidine (His₆) tag, and the glutathione S-transferase (GST) fusion proteins, mouse SNAP23 (amino acids 1–210), rat VAMP2 (amino acids 1–96) were generated as described previously [17, 28]. Mouse HMunc18c (N-terminal His₆-tag), HTMunc18c (N-terminal His₆-tag, TEV cleavage site, referred to as detagged Munc18c after the His tag is removed) and HL-Munc18c (N-terminal His₆-tag, with a 53 amino acid linker) constructs were also prepared as described by Rehman *et al.* [39]. The 53 amino acid linker has the following sequence: MSPIDPMGHHHHHHGRRASV AAGILVPRGSPGLDGIYARGIQASMAAGFG. For production of T4L fusion constructs, a synthetic gene for T4L (amino acids 1–164) was purchased from GeneArt® Gene Synthesis (Life Technologies, Carlsbad, CA) and cloned into the pET20b vector using the *HindIII* and *XhoI* restriction sites. The cytoplasmic Sx4 constructs (amino acids 1–275 and 30–275) were subsequently ligated into the pET20b-T4L vector between the *NdeI* and *HindIII* sites, resulting in the constructs designated Sx4₁₋₂₇₅-T4L-His and Sx4₃₀₋₂₇₅-T4L-His. Constructs containing a TEV cleavage site were generated by ligation independent cloning (LIC) [46]. TEV cleavage was required to produce de-tagged protein for the analysis of the interaction between unbound Sx4 and Munc18c, and unbound Sx4 and SNARE proteins. To generate constructs with an N-terminal cleavable His-tag, a ligation independent cloning (LIC) strategy was used [46]. For this, each fragment i.e. Sx4₁₋₂₇₅, Sx4₁₋₂₇₅-T4L, Sx4₁₋₂₉₈-TMD or Munc18c was PCR amplified using specific forward (5' -CAGGGCGCCAT**GCGGACAGGACCCATGAGTTGAGGC**-3') and reverse (5' -GACCCGACGCGGT**AAGTGAGCTCCAGGTTTTTATACGCAT**-3') primers containing LIC overhangs (in bold). The PCR product was then treated with T4-polymerase. T4 polymerase treated DNA was ligated to a LIC vector (pMCSG7 vector digested with *SspI* restriction enzyme). The LIC vector pMCSG7 encodes an N-terminal leader sequence containing a His₆ fusion tag and a TEV protease site (EXXYXQG/S). The plasmid was isolated and the sequence confirmed (Australian Genome Research Facility, University of Queensland).

To generate HT-Sx4-TMD a synthetic gene encoding full length Sx4-TMD (mouse, amino acids 1–298) was purchased from GenScript® (Piscataway, NJ) and cloned into a LIC vector with an N-terminal His₆ affinity tag as described above.

Production of soluble Sx, SNAP23, VAMP2 and Munc18 constructs

Munc18c proteins were expressed in *E. coli* and purified as described previously [39], with the following changes. Tris was replaced with 50 mM phosphate (pH 8.0) in all purification buffers. Cell pellet from 1 L of cells (OD ~18) was lysed using 500 mg lysozyme in lysis buffer (300 mL) at room temperature. The soluble forms of Sx4 proteins and its T4L fusions were expressed in *E. coli* and purified using the methods described for Sx4 previously [17, 28]. To remove the His₆-tag, proteins eluted after immobilized metal ion affinity chromatography (IMAC) with TALON™ Co²⁺ resin were mixed with TEV protease (A₂₈₀ ratio of 1:100,

protease: protein) and incubated overnight at 4°C. The following day, the protein was subjected to a reverse IMAC step and cleaved protein collected in the flow-through was further purified on a size exclusion chromatography column (SEC) Superdex S200 16/60 using an ÄKTA FPLC system (GE Healthcare, Little Chalfont, UK). An additional serine residue remained at the N-terminus of Sx4 and Munc18c proteins after TEV protease treatment (Fig 1B). GST-cleaved SNAP23 and VAMP2 were produced and purified as described previously [28]. Briefly proteins were lysed in lysis buffer (25 mM TrisCl, pH7.5, 150 mM NaCl, 0.5% Triton-X 100, 2 mM βME). The lysate was subsequently cleared by centrifugation and incubated with GSH-agarose resin (Thermo-Fisher Scientific, Massachusetts, USA) for 2 hrs. The beads were then washed with wash buffer (25 mM TrisCl, pH7.5, 150 mM NaCl, 2 mM βME) prior to treatment with thrombin to cleave the GST affinity tag. Cleaved protein was further purified by anion exchange chromatography on a MonoQ HR 5/5 column (GE Healthcare, Little Chalfont, UK) for SNAP23 and by cation exchange chromatography on a MonoS HR 5/5 column (GE Healthcare, Little Chalfont, UK) for VAMP2 and VAMP2 E78C.

Production of HT-Sx4₁₋₂₉₈-TMD

A single colony was picked from freshly transformed HT-Sx4₁₋₂₉₈-TMD in Lemo21 (DE3) cells (New England, BioLabs Inc., Ipswich, MA), and used to inoculate 200 mL LB containing antibiotics (50 μg/mL kanamycin). Cultures were incubated overnight at 37°C with shaking and then used to inoculate several 1 L cultures containing appropriate antibiotics. Cells were incubated at 37°C with shaking (200 rpm) and induced with 1 mM IPTG and 0.25 mM L-rhamnose at an OD₆₀₀ of 0.6. Growth was continued for 18–20 h at 22°C with shaking. Cells were harvested by centrifugation (5000g, 4°C). For protein purification, cells were homogenized in a 1:10 ratio (wet cell pellet mass: buffer) using lysis buffer (25 mM Tris-Cl pH 7.5, 150 mM NaCl, 2 mM βME, 10 mM MgCl₂, 1% (v/v) Triton X-100, 1% (w/v) DDM (Glycon Biochemical, Luckenwalde, Germany) 12,500–14,000 units DNase (Roche, Basel, Switzerland), 100 μL of Bacterial Protease Inhibitor (Bio Pioneer, Inc., San Diego, CA). Cells were then lysed by addition of lysozyme (Astral Scientific, Gympie, NSW, Australia) to a final concentration of 200 μg/mL followed by incubation at 4°C for 2 h. Insoluble protein and cell debris were removed by centrifugation using a Beckman Optima™ L-100 XP ultracentrifuge (45Ti rotor, 30,000g, 40 min, 4°C). The soluble membrane fraction was mixed with pre-equilibrated TALON™ Co²⁺ beads and incubated at 4°C. After extensive washing (25 mM Tris-Cl pH 7.5, 200 mM NaCl, 10% (v/v) glycerol, 0.1% (w/v) β-DDM with 10 mM imidazole, followed by buffer with 25 mM imidazole) the protein was eluted in buffer (25 mM Tris-Cl pH 7.5, 200 mM NaCl, 10% (v/v) glycerol, 0.1% (w/v) β-DDM, 300 mM imidazole) and further purified on Superdex 200 (G10/300) column pre-equilibrated with SEC buffer (25 mM Tris-Cl pH 7.5, 200 mM NaCl, 2 mM βME, 0.03% (w/v) DDM, 10% (v/v) glycerol) on an AKTA FPLC system (GE Healthcare, Little Chalfont, UK). To generate de-tagged protein, HT-Sx4₁₋₂₉₈-TMD eluted from the IMAC resin was mixed with TEV protease in a 1:10 ratio (A₂₈₀ ratio of protease: protein) and incubated while being buffer exchanged into 25 mM Tris-Cl pH 7.5, 200 mM NaCl, 2 mM βME, 0.03 (w/v) β-DDM, 10% (v/v) glycerol, 10 mM imidazole overnight at 4°C. A reverse-IMAC purification step was then used to separate the de-tagged membrane protein.

In vitro pull-down binding assays with immobilized Sx4 mutants or immobilized Munc18c

Two pull-down assays were used to assess Sx4 protein binding with Munc18c and SNAREs. In the first set of experiments, all Sx4 proteins (Sx4₁₋₂₇₅-His, Sx4₁₋₂₇₅-T4L-His or Sx4₃₀₋₂₇₅-T4L-His) (30 μg each, 4.7 μM (Sx4₁₋₂₇₅-His), 3.0 μM (Sx4₁₋₂₇₅-T4L-His) or 3.2 μM (Sx4₃₀₋₂₇₅-

T4L-His) in a volume of 200 μL) were immobilized onto TALON™ Co^{2+} beads via their C-terminal His₆-tag fusion. Beads bound with Sx4 proteins were mixed with purified de-tagged Munc18c protein (50 μg , 3.7 μM), prepared by TEV protease treatment of HTMunc18c at 4°C for 2 h to assess binary complex formation. For quaternary complexes, beads with immobilized Munc18c/Sx4-His (Sx4₁₋₂₇₅-His or Sx4₁₋₂₇₅-T4L-His) complex were incubated with GST-cleaved SNAP23/VAMP2 (40 μg) overnight at 4°C. Binding buffer contained 25 mM Tris-Cl pH 7.5, 150 mM NaCl, 10 mM imidazole, 0.1% (v/v) Triton X-100, 10% (v/v) glycerol, 2 mM βME , 2 mM AEBF. The beads were washed extensively with binding buffer (excluding 2 mM AEBF) and the bound proteins analyzed by SDS-PAGE and Coomassie Blue staining. The Sx4-T4L fusion proteins, Sx4₁₋₂₇₅-T4L-His and Sx4₃₀₋₂₇₅-T4L-His were used to assess binary complex formation (Munc18c/Sx4), whereas for quaternary complex (Munc18c/SNARE) formation only the Sx4₁₋₂₇₅-T4L-His construct was used.

In a second set of experiments, HL-Munc18c (20 μg , 1.4 μM in a volume of 200 μL) was first immobilized on TALON™ Co^{2+} beads. Beads were incubated separately with de-tagged Sx4₁₋₂₇₅, Sx4₁₋₂₇₅-T4L or Sx4₁₋₂₉₈-TMD (50 μg , 21.7 μM) for 4 h in the binding buffer described above and washed with binding buffer. For quaternary complex formation, the beads (containing HL-Munc18c/Sx4 binary complexes or Sx4 proteins without HL-Munc18c for the control) were mixed with purified SNAP23 (100 μg , 21.7 μM) and VAMP2 (80 μg , 31.7 μM) proteins and incubated overnight at 4°C using each of the three de-tagged Sx4 proteins (Sx4₁₋₂₇₅, Sx4₁₋₂₇₅-T4L and Sx4₁₋₂₉₈-TMD) in binding buffer. Unbound and non-specific proteins were removed by washing with binding buffer and the level of binding was analyzed by SDS-PAGE. Each binding assay was repeated at least three times to confirm the results. Protein concentrations were measured using the Bio-Rad protein assay with bovine serum albumin used as a standard.

Nonspecific binding of detagged proteins was assessed by incubating the individual proteins overnight either with T4-Lysozyme-His (20 μg) immobilized onto beads (S3 Fig) or with beads alone (Fig 4 (for Munc18c)) and Fig 5 (for Sx4₁₋₂₇₅, Sx4₁₋₂₉₈-TMD, or Sx4₁₋₂₇₅-T4L)).

Isothermal titration calorimetry (ITC)

ITC experiments were carried out at 298 K using an iTC200 (Malvern Instruments Ltd., Malvern, United Kingdom). The proteins were buffer exchanged in ITC buffer (25 mM HEPES pH 8.0, 200 mM NaCl, 10% (v/v) glycerol and 2 mM $\beta\text{-ME}$) by gel filtration prior to ITC experiments. Sx4₁₋₂₇₅-T4L-His or Sx4₃₀₋₂₇₅-T4L-His at a concentration of 200–250 μM was titrated into 20–40 μM of HMunc18c in the cell. Injection volumes of 2.5 μL were used for all titrations. The heat released was measured and integrated using the Microcal Origin 7.0 program with a single site binding model to calculate the equilibrium association constant K_a ($= 1/K_d$), enthalpy of binding (ΔH) and the stoichiometry (n). The Gibbs free energy (ΔG) was calculated using the equation:

$$\Delta G = -RT \ln(K_a)$$

Binding entropy (ΔS) was calculated by

$$\Delta G = \Delta H - T\Delta S.$$

To determine the average standard error of the mean (SEM) values of binding affinities, four experiments were performed for each set of samples.

Bio-layer interferometry

The binding kinetics of Sx4₁₋₂₇₅ or Sx4₁₋₂₇₅-T4L for their interaction with Munc18c was determined by bio-layer interferometry using a BLITZ[®] system (ForteBio, Menlo Park, CA). In the

first series of experiments C-terminally His-tagged Sx4 constructs (200–400 nM) were loaded onto Ni-NTA biosensors until a binding height of ~ 1 nm was reached. Sx4 immobilized sensors were dipped into a dilution series of de-tagged Munc18c at concentrations of 25, 50, 100, 200 and 400 nM for Sx4₁₋₂₇₅-His and 10, 25, 50, 100, 200 and 400 nM for Sx4₁₋₂₇₅-T4L-His immobilized biosensors. The association reaction was allowed to proceed for 60–100 s and the dissociation reaction for 120–180 s. Experiments were conducted with a shaking speed of 2200 rpm in 25 mM Tris-Cl pH 7.5, 150 mM NaCl, 10 mM imidazole, 0.1% (v/v) TX-100, 10% (v/v) glycerol and 2 mM βME buffer. We were unable to assess the association of Munc18c with Sx4₁₋₂₉₈-TMD using biolayer interferometry because of poor yield and purity of C-terminally His-tagged full-length Sx4 protein.

In a second series of experiments HL-Munc18c was immobilized onto Ni-NTA biosensors until a binding height of ~ 1 nm was achieved. The biosensors were dipped into a concentration series of 25, 50, 100, 200 and 400 nM for detagged Sx4₁₋₂₇₅ and 25, 50, 100, 200 and 400 nM for detagged Sx4₁₋₂₇₅-T4L. The association reaction was for 100 s and dissociation was followed for 120 s. Experiments were conducted three times using at least two replicates from independently prepared samples and the data were fitted to an interaction with 1:1 stoichiometry using BLItz[®] Pro Software.

Labeling proteins for fluorescence experiments

Cysteine variants were prepared using QuikChange Mutagenesis (Stratagene, San Diego, CA). These were (i) Sx4₁₋₂₇₅-His and Sx4₁₋₂₇₅-T4L (native C141 rather than C141S), to study Munc18c/Sx4 kinetics and (ii) GST cleaved VAMP2 E78C to study SNARE ternary complex formation. Site-specific labeling of these two proteins was performed using the thiol reactive Alexa488 C₅ Maleimide dye according to the manufacturer's instructions (Alexa Fluor[®] 488, Life Technologies, Carlsbad CA). Briefly, purified protein (200 μM) was mixed with dye to give a final dye concentration of 1 mM (in DMSO, final concentration 10% v/v) and incubated for 2–3 h in the dark at room temperature. Unbound dye was removed by sequentially passing the protein-dye mix through two equilibrated desalting PD10 columns (GE Healthcare, Little Chalfont, UK). The protein was collected and concentrated to the desired concentration. The absorbance of labeled protein at 280 nm (A_{280}) and 494 nm (A_{494}) was measured using a 1 cm cuvette in a nanodrop, and the degree of labeling was then calculated as recommended by the supplier:

$$\text{degree of protein labeling} = \frac{A_{494} \cdot \epsilon_{\text{protein}}}{\epsilon_{\text{Alexa-488}} (A_{280} - 0.11 \times A_{494})} \times 100\%$$

where the approximate molar extinction coefficient of Alexa 488 ($\epsilon_{\text{Alexa-488}}$) at 494 nm is 71000 M⁻¹cm⁻¹. The molar extinction coefficient of the protein ($\epsilon_{\text{protein}}$) was calculated from each protein sequence using the ExPASy ProtParam server [47]. In all cases, the degree of labeling was calculated to be greater than 90%.

Fluorescence anisotropy measurements

Long-time base-fluorescence anisotropy measurements were performed at 25°C in 1 mL quartz cuvettes (Hellma, Mullheim, Germany) without stirring on a Fluoromax-4 spectrofluorometer fitted with polarizers of L-geometry and slits set at 4 nm (Jobin Yvon Inc., Edison, NJ). The experiments were carried out in a buffer containing 25 mM HEPES pH 8.0, 200 mM NaCl, 1 mM TCEP and 2% (w/v) glycerol. The Alexa488 fluorophore was excited at 488 nm and emission was observed at 515 nm. Fluorescence anisotropy (r) was determined as:

$$\langle r \rangle = I_{VV} - G I_{VH} / I_{VV} - 2GI_{VH}$$

where I represents the fluorescence intensity, and the first subscript letter indicates the direction of excited light and second subscript shows the emitted light. The intensities of vertically (V) and horizontally (H) polarized emission light after excitation were measured. The “G-factor” G was defined as:

$$G = I_{VH}/I_{HH}$$

Primary data analysis was performed with the programs Graffit 5.0 (Erithacus software) and Fluorescence implementation (Jobin Yvon Inc., Edison, NJ) of the Origin7.0 software (Origin lab Corporation, Northampton, MA). Experiments investigating the kinetics of the interaction between Sx4₁₋₂₇₅-His or Sx4₁₋₂₇₅-T4L-His and HMunc18c were performed once at each concentration of HMunc18c. The experiments investigating the formation of the SNARE complex used Alexa488-labeled VAMP2 (GST-cleaved), GST cleaved SNAP23, and the same Sx4 and Munc18c proteins, and were each performed at least three times. All spectra were corrected for background fluorescence from buffer.

To confirm the specificity of binding and complex formation, all proteins (Sx4₁₋₂₇₅-His, Sx4₁₋₂₇₅-T4L-His, HMunc18c, GST-cleaved SNAP23) were tested individually for their ability to bind Alexa488-labeled VAMP2 (GST cleaved). The change in anisotropy was monitored and showed that none of these proteins interacted on their own with VAMP2-Alexa488 under the given experimental conditions. We were unable to assess the association of HMunc18c with the full length Sx4₁₋₂₉₈-TMD-His using fluorescence anisotropy because the presence of detergent prevented a stable baseline under the same conditions.

The global fit for the anisotropy data was calculated using the Dynafit 4.0 program. During the fitting procedure (1:1 complex), the concentration of proteins was allowed to vary and then checked against the anticipated value. The script used in global calculations of kinetic parameters for the interaction of Munc18c with Sx4 or Sx4-T4L is provided as supporting information ([S1 Text](#)).

Supporting information

S1 Table. Thermodynamic parameters for the HMunc18c:Sx4₁₋₂₇₅-T4L-His and HMunc18c:Sx4₃₀₋₂₇₅-T4L-His interactions determined using isothermal titration calorimetry. Values are shown as mean ± SEM from four independent experiments. NB indicates no binding was detected.
(PDF)

S1 Fig. ITC data for the Interaction between HMunc18c and Sx4₁₋₂₇₅-T4L-His and HMunc18c and Sx4₃₀₋₂₇₅-T4L-His. The upper panel depicts the raw ITC data while the lower panel is the integrated normalized data. Experiments were conducted at 298 K where Sx4₁₋₂₇₅-T4L-His or Sx4₃₀₋₂₇₅-T4L-His (200–250 μM) was titrated into HMunc18c (20–40 μM) in the cell with an injection volume of 2.5 μL.
(EPS)

S2 Fig. Bio-layer interferometry data for interaction between Sx4 constructs and Munc18c (A) immobilized Sx4₁₋₂₇₅-His with Munc18c in solution, (B) immobilized Sx4₁₋₂₇₅-T4L-His with Munc18c in solution, (C) HLMunc18c immobilized with Sx4₁₋₂₇₅ in solution and (D) HLMunc18c immobilized with Sx4₁₋₂₇₅-T4L in solution. The black line denotes the fitting for a 1:1 binding model.
(EPS)

S3 Fig. Immobilized T4L does not interact with (detagged) Sx4, Munc18c, SNAP23 or VAMP2. Coomassie Blue stained SDS-PAGE gels. Lanes labeled INPUTS show the protein

samples used in the experiments and the T4L-His protein immobilized on resin. Lanes labeled Controls show the interaction between T4L and the detached SNARE and Munc18c (M18c) proteins.

(EPS)

S1 Text. Script for global calculation of kinetic parameters by fluorescence anisotropy.

(PDF)

Acknowledgments

We acknowledge with thanks the initial cloning of Sx4-T4L constructs by Dr Niranjali Gamage. We are very grateful to Dr Julia K. Archbold for critical comments and editing this manuscript.

Author Contributions

Conceptualization: Asma Rehman, Andrew E. Whitten, Michelle P. Christie, Jennifer L. Martin.

Data curation: Asma Rehman, Zakir Tnimov, Michelle P. Christie.

Formal analysis: Asma Rehman, Shu-Hong Hu, Zakir Tnimov, Andrew E. Whitten, Gordon J. King, Russell J. Jarrott, Suzanne J. Norwood, Brett M. Collins, Michelle P. Christie, Jennifer L. Martin.

Funding acquisition: Andrew E. Whitten, Kirill Alexandrov, Brett M. Collins, Jennifer L. Martin.

Investigation: Asma Rehman, Shu-Hong Hu, Zakir Tnimov, Andrew E. Whitten, Gordon J. King, Russell J. Jarrott, Michelle P. Christie.

Methodology: Asma Rehman, Shu-Hong Hu, Zakir Tnimov, Andrew E. Whitten, Michelle P. Christie, Jennifer L. Martin.

Project administration: Andrew E. Whitten, Michelle P. Christie, Jennifer L. Martin.

Resources: Kirill Alexandrov, Brett M. Collins, Jennifer L. Martin.

Supervision: Shu-Hong Hu, Andrew E. Whitten, Suzanne J. Norwood, Kirill Alexandrov, Brett M. Collins, Michelle P. Christie, Jennifer L. Martin.

Validation: Shu-Hong Hu, Zakir Tnimov, Andrew E. Whitten, Russell J. Jarrott, Michelle P. Christie, Jennifer L. Martin.

Visualization: Asma Rehman, Shu-Hong Hu, Zakir Tnimov, Andrew E. Whitten, Michelle P. Christie.

Writing – original draft: Asma Rehman, Shu-Hong Hu, Zakir Tnimov, Andrew E. Whitten, Russell J. Jarrott, Suzanne J. Norwood, Brett M. Collins, Michelle P. Christie, Jennifer L. Martin.

Writing – review & editing: Shu-Hong Hu, Andrew E. Whitten, Gordon J. King, Michelle P. Christie, Jennifer L. Martin.

References

1. Weber T, Zemelman BV, McNew JA, Westermann B, Gmachl M, Parlati F, et al. SNAREpins: minimal machinery for membrane fusion. *Cell*. 1998; 92(6):759–72. PMID: [9529252](https://pubmed.ncbi.nlm.nih.gov/9529252/).

2. Jahn R, Scheller RH. SNAREs—engines for membrane fusion. *Nat Rev Mol Cell Biol.* 2006; 7(9):631–43. <https://doi.org/10.1038/nrm2002> PMID: 16912714.
3. Gao Y, Zorman S, Gundersen G, Xi Z, Ma L, Sirinakis G, et al. Single reconstituted neuronal SNARE complexes zipper in three distinct stages. *Science.* 2012; 337(6100):1340–3. <https://doi.org/10.1126/science.1224492> PMID: 22903523; PubMed Central PMCID: PMC3677750.
4. Toonen RF, Verhage M. Vesicle trafficking: pleasure and pain from SM genes. *Trends in Cell Biol.* 2003; 13(4):177–86. Epub 2003/04/02. PMID: 12667755.
5. Archbold JK, Whitten AE, Hu SH, Collins BM, Martin JL. SNARE-ing the structures of Sec1/Munc18 proteins. *Curr Opin Struct Biol.* 2014; 29:44–51. Epub 2014/10/06. <https://doi.org/10.1016/j.sbi.2014.09.003> PMID: 25282382.
6. Rea S, Martin LB, McIntosh S, Macaulay SL, Ramsdale T, Baldini G, et al. Syndet, an adipocyte target SNARE involved in the insulin-induced translocation of GLUT4 to the cell surface. *J Biol Chem.* 1998; 273(30):18784–92. Epub 1998/07/21. PMID: 9668052.
7. Tellam JT, McIntosh S, James DE. Molecular identification of two novel Munc-18 isoforms expressed in non-neuronal tissues. *J Biol Chem.* 1995; 270(11):5857–63. PMID: 7890715.
8. Martin LB, Shewan A, Millar CA, Gould GW, James DE. Vesicle-associated membrane protein 2 plays a specific role in the insulin-dependent trafficking of the facilitative glucose transporter GLUT4 in 3T3-L1 adipocytes. *J Biol Chem.* 1998; 273(3):1444–52. Epub 1998/01/27. PMID: 9430681.
9. Han L, Jiang T, Han GA, Malintan NT, Xie L, Wang L, et al. Rescue of Munc18-1 and -2 double knock-down reveals the essential functions of interaction between Munc18 and closed syntaxin in PC12 cells. *Mol Biol Cell.* 2009; 20(23):4962–75. Epub 2009/10/09. <https://doi.org/10.1091/mbc.E09-08-0712> PMID: 19812250; PubMed Central PMCID: PMC2785739.
10. Verhage M, Maia AS, Plomp JJ, Brussaard AB, Heeroma JH, Vermeer H, et al. Synaptic assembly of the brain in the absence of neurotransmitter secretion. *Science.* 2000; 287(5454):864–9. Epub 2000/02/05. PMID: 10657302.
11. Hata Y, Slaughter CA, Südhof TC. Synaptic vesicle fusion complex contains unc-18 homologue bound to syntaxin. *Nature.* 1993; 366(6453):347–51. Epub 1993/11/25. <https://doi.org/10.1038/366347a0> PMID: 8247129.
12. Südhof TC, Rizo J. Synaptic vesicle exocytosis. *Cold Spring Harbour Perspect Biol.* 2011; 3(12). Epub 2011/10/27. <https://doi.org/10.1101/cshperspect.a005637> PMID: 22026965; PubMed Central PMCID: PMC3225952.
13. Rizo J, Rosenmund C. Synaptic vesicle fusion. *Nat Struct Mol Biol.* 2008; 15(7):665–74. PMID: 18618940
14. Deak F, Xu Y, Chang WP, Dulubova I, Khvotchev M, Liu XR, et al. Munc18-1 binding to the neuronal SNARE complex controls synaptic vesicle priming. *J Cell Biol.* 2009; 184(5):751–64. <https://doi.org/10.1083/jcb.200812026> PMID: 19255244
15. Burkhardt P, Stegmann CM, Cooper B, Kloepper TH, Imig C, Varoqueaux F, et al. Primordial neurosecretory apparatus identified in the choanoflagellate *Monosiga brevicollis*. *Proc Natl Acad Sci U S A.* 2011; 108(37):15264–9. <https://doi.org/10.1073/pnas.1106189108> PMID: 21876177; PubMed Central PMCID: PMC3174607.
16. Meijer M, Burkhardt P, de Wit H, Toonen RF, Fasshauer D, Verhage M. Munc18-1 mutations that strongly impair SNARE-complex binding support normal synaptic transmission. *EMBO J.* 2012; 31(9):2156–68. <https://doi.org/10.1038/emboj.2012.72> PMID: 22446389; PubMed Central PMCID: PMC3343470.
17. Christie MP, Whitten AE, King GJ, Hu SH, Jarrott RJ, Chen KE, et al. Low-resolution solution structures of Munc18:Syntaxin protein complexes indicate an open binding mode driven by the Syntaxin N-peptide. *Proc Natl Acad Sci U S A.* 2012; 109(25):9816–21. <https://doi.org/10.1073/pnas.1116975109> PMID: 22670057; PubMed Central PMCID: PMC3382502.
18. Burkhardt P, Hattendorf DA, Weis WI, Fasshauer D. Munc18a controls SNARE assembly through its interaction with the syntaxin N-peptide. *EMBO J.* 2008; 27(7):923–33. <https://doi.org/10.1038/emboj.2008.37> PMID: 18337752; PubMed Central PMCID: PMC2323264.
19. Colbert KN, Hattendorf DA, Weiss TM, Burkhardt P, Fasshauer D, Weis WI. Syntaxin1a variants lacking an N-peptide or bearing the LE mutation bind to Munc18a in a closed conformation. *Proc Natl Acad Sci U S A.* 2013; 110(31):12637–42. <https://doi.org/10.1073/pnas.1303753110> PMID: 23858467; PubMed Central PMCID: PMC3732934.
20. Ma C, Li W, Xu Y, Rizo J. Munc13 mediates the transition from the closed syntaxin-Munc18 complex to the SNARE complex. *Nat Struct Mol Biol.* 2011; 18(5):542–9. Epub 2011/04/19. <https://doi.org/10.1038/nsmb.2047> PMID: 21499244; PubMed Central PMCID: PMC3087822.

21. Shen JS, Rathore SS, Khandan L, Rothman JE. SNARE bundle and syntaxin N-peptide constitute a minimal complement for Munc18-1 activation of membrane fusion. *J Cell Biol.* 2010; 190(1):55–63. <https://doi.org/10.1083/jcb.201003148> PMID: 20603329
22. Dulubova I, Khvotchev M, Liu S, Huryeva I, Südhof T. C., Rizo J. Munc18-1 binds directly to the neuronal SNARE complex. *Proc Natl Acad Sci U S A.* 2007; 104(8):2697–702. Epub 2007/02/16. 0611318104 [pii] <https://doi.org/10.1073/pnas.0611318104> PMID: 17301226; PubMed Central PMCID: PMC1815244.
23. Rathore SS, Bend EG, Yu HJ, Hammarlund M, Jorgensen EM, Shen JS. Syntaxin N-terminal peptide motif is an initiation factor for the assembly of the SNARE-Sec1/Munc18 membrane fusion complex. *Proc Natl Acad Sci U S A.* 2010; 107(52):22399–406. <https://doi.org/10.1073/pnas.1012997108> PMID: 21139055
24. Rodkey TL, Liu S, Barry M, McNew JA. Munc18a Scaffolds SNARE Assembly to Promote Membrane Fusion. *Mol Biol Cell.* 2008; 19(12):5422–34. <https://doi.org/10.1091/mbc.E08-05-0538> PMID: 18829865
25. Hu S-H, Christie MP, Saez NJ, Latham CF, Jarrott R, Lua LH, et al. Possible roles for Munc18-1 domain 3a and Syntaxin1 N-peptide and C-terminal anchor in SNARE complex formation. *Proc Natl Acad Sci U S A.* 2011; 108(3):1040–5. Epub 2011/01/05. <https://doi.org/10.1073/pnas.0914906108> PMID: 21193638; PubMed Central PMCID: PMC3024693.
26. Malintan NT, Nguyen TH, Han L, Latham CF, Osborne SL, Wen PJ, et al. Abrogating Munc18-1-SNARE complex interaction has limited impact on exocytosis in PC12 cells. *J Biol Chem.* 2009; 284(32):21637–46. Epub 2009/06/02. <https://doi.org/10.1074/jbc.M109.013508> PMID: 19483085; PubMed Central PMCID: PMC2755887.
27. Yu H, Rathore SS, Lopez JA, Davis EM, James DE, Martin JL, et al. Comparative studies of Munc18c and Munc18-1 reveal conserved and divergent mechanisms of Sec1/Munc18 proteins. *Proc Natl Acad Sci U S A.* 2013; 110(35):E3271–80. <https://doi.org/10.1073/pnas.1311232110> PMID: 23918365.
28. Latham CF, Lopez JA, Hu S-H, Gee CL, Westbury E, Blair DH, et al. Molecular dissection of the Munc18c/syntaxin4 interaction: Implications for regulation of membrane trafficking. *Traffic.* 2006; 7(10):1408–19. <https://doi.org/10.1111/j.1600-0854.2006.00474.x> PMID: 16899085
29. Gerber SH, Rah JC, Min SW, Liu XR, de Wit H, Dulubova I, et al. Conformational switch of syntaxin-1 controls synaptic vesicle fusion. *Science.* 2008; 321(5895):1507–10. <https://doi.org/10.1126/science.1163174> PMID: 18703708
30. Stein A, Weber G, Wahl MC, Jahn R. Helical extension of the neuronal SNARE complex into the membrane. *Nature.* 2009; 460(7254):525–8. Epub 2009/07/03. <https://doi.org/10.1038/nature08156> PMID: 19571812; PubMed Central PMCID: PMC3108252.
31. Peng R, Guetg C, Abellan E, Fussenegger M. Munc18b regulates core SNARE complex assembly and constitutive exocytosis by interacting with the N-peptide and the closed-conformation C-terminus of syntaxin 3. *Biochem J.* 2010; 431(3):353–61. <https://doi.org/10.1042/BJ20100145> PMID: 20695848
32. Brandie FM, Aran V, Verma A, McNew JA, Bryant NJ, Gould GW. Negative regulation of syntaxin4/SNAP-23/VAMP2-mediated membrane fusion by Munc18c in vitro. *PLoS One.* 2008; 3(12):e4074. <https://doi.org/10.1371/journal.pone.0004074> PMID: 19116655; PubMed Central PMCID: PMC2605266.
33. Shen J, Tareste DC, Paumet F, Rothman JE, Melia TJ. Selective activation of cognate SNAREpins by Sec1/Munc18 proteins. *Cell.* 2007; 128(1):183–95. Epub 2007/01/16. S0092-8674(06)01610-2 [pii] <https://doi.org/10.1016/j.cell.2006.12.016> PMID: 17218264.
34. Schollmeier Y, Krause JM, Kreye S, Malsam J, Sollner TH. Resolving the function of distinct Munc18-1/SNARE protein interaction modes in a reconstituted membrane fusion assay. *J Biol Chem.* 2011; 286(35):30582–90. Epub 2011/07/07. M111.269886 [pii] <https://doi.org/10.1074/jbc.M111.269886> PMID: 21730064; PubMed Central PMCID: PMC3162418.
35. Diao J, Su Z, Lu X, Yoon T-Y, Shin Y-K, Ha T. Single-Vesicle Fusion Assay Reveals Munc18-1 Binding to the SNARE Core Is Sufficient for Stimulating Membrane Fusion. *ACS Chem Neuroscience.* 2010; 1(3):168–74. <https://doi.org/10.1021/cn900034p> PMID: 20300453
36. Tareste D, Shen J, Melia TJ, Rothman JE. SNAREpin/Munc18 promotes adhesion and fusion of large vesicles to giant membranes. *Proc Natl Acad Sci U S A.* 2008; 105(7):2380–5. Epub 2008/02/13. <https://doi.org/10.1073/pnas.0712125105> PMID: 18268324; PubMed Central PMCID: PMC2268145.
37. Rehman A, Archbold JK, Hu S-H, Norwood SJ, Collins BM, Martin JL. Reconciling the regulatory role of Munc18 proteins in SNARE-complex assembly. *IUCrJ.* 2014; 1(6):505–13. <https://doi.org/10.1107/S2052252514020727> PMID: 25485130
38. Cherezov V, Rosenbaum DM, Hanson MA, Rasmussen S, Ren GF, Thian FS, et al. High-resolution crystal Structure of an engineered human b2-adrenergic G protein-coupled receptor. *Science.* 2007; 318(5854):1258–65. <https://doi.org/10.1126/science.1150577> PMID: 17962520

39. Rehman A, Jarrott R, Whitten AE, King GJ, Hu S-H, Christie MP, et al. Milligram quantities of homogeneous recombinant full-length mouse Munc18c from *Escherichia coli* cultures. PLoS One. 2013; 8: e83499. <https://doi.org/10.1371/journal.pone.0083499> PMID: 24391775
40. Aran V, Brandie FM, Boyd AR, Kantidakis T, Rideout EJ, Kelly SM, et al. Characterization of two distinct binding modes between syntaxin 4 and Munc18c. Biochem J. 2009; 419(3):655–60. <https://doi.org/10.1042/BJ20082293> PMID: 19193195.
41. Rickman C, Medine CN, Bergmann A, Duncan RR. Functionally and spatially distinct modes of Munc18-syntaxin 1 interaction. J Biol Chem. 2007; 282(16):12097–103. Epub 2007/02/01. M700227200 [pii] <https://doi.org/10.1074/jbc.M700227200> PMID: 17264080; PubMed Central PMCID: PMC1891423.
42. Misura KM, Scheller RH, Weis WI. Three-dimensional structure of the neuronal-Sec1-syntaxin 1a complex. Nature. 2000; 404(6776):355–62. <https://doi.org/10.1038/35006120> PMID: 10746715.
43. Chen X, Lu J, Dulubova I, Rizo J. NMR analysis of the closed conformation of syntaxin-1. J Biomol NMR. 2008; 41(1):43–54. <https://doi.org/10.1007/s10858-008-9239-1> PMID: 18458823; PubMed Central PMCID: PMC2685195.
44. Liang B, Kiessling V, Tamm LK. Prefusion structure of syntaxin-1A suggests pathway for folding into neuronal trans-SNARE complex fusion intermediate. Proc Natl Acad Sci U S A. 2013; 110(48):19384–9. <https://doi.org/10.1073/pnas.1314699110> PMID: 24218570.
45. Zhou P, Bacaj T, Yang X, Pang ZP, Südhof TC. Lipid-anchored SNAREs lacking transmembrane regions fully support membrane fusion during neurotransmitter release. Neuron. 2013; 80(2):470–83. <https://doi.org/10.1016/j.neuron.2013.09.010> PMID: 24120845.
46. Stols L, Gu M, Dieckman L, Raffin R, Collart FR, Donnelly MI. A new vector for high-throughput, ligation-independent cloning encoding a tobacco etch virus protease cleavage site. Protein Exp Purif. 2002; 25(1):8–15. <https://doi.org/10.1006/prep.2001.1603> PMID: 12071693.
47. Gasteiger E, Gattiker A., Duvaud S., Wilkins M.R., Appel R.D., Bairoch A. Protein Identification and Analysis Tools on the ExPASy Server. Walker John M (ed): The Proteomics Protocols Handbook Humana Press 2005:571–607.



Minerva Access is the Institutional Repository of The University of Melbourne

Author/s:

Rehman, A; Hu, S-H; Tnimov, Z; Whitten, AE; King, GJ; Jarrott, RJ; Norwood, SJ;
Alexandrov, K; Collins, BM; Christie, MP; Martin, JL

Title:

The nature of the Syntaxin4 C-terminus affects Munc18c-supported SNARE assembly

Date:

2017-08-25

Citation:

Rehman, A; Hu, S-H; Tnimov, Z; Whitten, AE; King, GJ; Jarrott, RJ; Norwood, SJ;
Alexandrov, K; Collins, BM; Christie, MP; Martin, JL, The nature of the Syntaxin4 C-terminus
affects Munc18c-supported SNARE assembly, PLOS ONE, 2017, 12 (8)

Persistent Link:

<http://hdl.handle.net/11343/221622>

File Description:

Published version